COILING DIRECTION OF THE PLANKTIC FORAMINIFER *GLOBOROTALIA TRUNCATULINOIDES* AS A PROXY FOR RECONSTRUCTING UPPER OCEAN HYDROGRAPHY IN THE NORTH ATLANTIC DURING THE MID-PLEISTOCENE CLIMATE TRANSITION

by

Andrew D. Caldwell

A thesis submitted to the Faculty of the University of Delaware in partial fulfillment of the requirements for the degree of Master of Science in Marine Studies

Spring 2018

COILING DIRECTION OF THE PLANKTIC FORAMINIFER

***GLOBOROTALIA TRUNCATULINOIDES* AS A PROXY FOR**

RECONSTRUCTING UPPER OCEAN HYDROGRAPHY IN THE NORTH

ATLANTIC DURING THE MID-PLEISTOCENE CLIMATE TRANSITION

by

Andrew D. Caldwell

Approved: _____
  Katharina Billups, Ph.D.
  Professor in charge of thesis on behalf of the Advisory Committee

Approved: _____
  Mark Moline, Ph.D.
  Director of the School of Marine Science and Policy

Approved: _____
  Estella Atekwana, Ph.D.
  Dean of the College of Earth, Ocean and Environment

Approved: _____
  Ann L. Ardis, Ph.D.
  Senior Vice Provost for Graduate and Professional Education

ACKNOWLEDGMENTS

TABLE OF CONTENTS

LIST OF FIGURES

ABSTRACT

This study uses the coiling direction of the planktic foraminifer *Globorotalia truncatulinoides* as a proxy for reconstructing past changes in upper ocean hydrography in the northwestern subtropical Atlantic Ocean during the mid-Pleistocene climate transition (~0.4 – 1.2 Ma). The mid-Pleistocene transition is a time interval of interest because it encompasses the evolution of glacial-interglacial cycles from less severe, 41 kyr-paced glaciations to more severe, 100 kyr-paced glaciations, without any observable changes in corresponding orbital forcing. I hypothesize that the establishment and persistence of the more extreme glaciations characteristic of the current 100 kyr world was associated with changes in the hydrography of the subtropical North Atlantic and the related poleward heat transport, evident in the downcore coiling ratio of *G. truncatulinoides*. The Gulf Stream and surrounding North Atlantic current system transport a substantial amount of heat from the equator to the poles, and therefore have a significant climatic impact on large temporal and spatial scales. Here I test whether or not changes in subtropical gyre dynamics, particularly the relative strength and position of the Gulf Stream and subtropical gyre, played a role in contributing to the onset of the 100 kyr cycle. To do this, I will construct a record of downcore variations in the coiling direction of *G. truncatulinoides* spanning the mid-Pleistocene transition. Studies have shown that there are spatial and temporal

differences in the coiling direction of *G. truncatulinoides* through time as a result of changes in oceanic conditions; for example, sediments dominated by left coiling specimens characterize interglacial periods and deeper permanent thermoclines, while sediments dominated by right coiling specimens characterize glacial periods and shallower permanent thermoclines. Deeper permanent thermoclines are characteristic of interglacial periods due to enhanced flow of the subtropical gyre and Gulf Stream, and therefore greater poleward heat transport; these environmental conditions favor the left coiling variety of *G. truncatulinoides*. Conversely, shallow permanent thermoclines are characteristic of glacial periods due to reduced flow of the subtropical gyre and Gulf Stream, favoring the right coiling variety. There have been studies exploring the hydrography of the subtropical North Atlantic across parts of the mid-Pleistocene transition, but not necessarily across the entire interval. This study will provide valuable insight into the relative position of the Gulf Stream and the North Atlantic subtropical gyre across the mid-Pleistocene transition, exploring the implication of these features on oceanic heat transport.

Chapter 1

INTRODUCTION

In the 1920s, Milutin Milankovic proposed that changes in Earth's planetary orbit influence the amount of solar radiation reaching different parts of the Earth through time (Milankovitch, 1920). This gave rise to research about these variations in Earth's planetary orbit, and how these variations have influenced Earth's climate throughout Earth's history. Specifically, the amount of solar insolation reaching the Earth is a dominant factor in the growth and decay of ice sheets during glaciations and deglaciations (Hays et al., 1976). Paleoclimatologists have been interested in the relationship between Milankovitch cycles, solar insolation, and Earth's climate through the past hundreds of thousands, and even millions of years, in order to gain a better understanding of the Earth's climate system (Hays et al., 1976; Pisias and Moore, 1981; Raymo et al., 1989; Ruddiman et al., 1989; Imbrie et al., 1993; Raymo et al., 1994; Mudelsee and Schulz, 1997; Weirauch et al., 2008).

The Pleistocene is the geologic time period from approximately 2.7 million years ago (Ma) to 11,700 years ago (the Holocene). It is known for cycles of glaciations (glacials) and deglaciations (interglacials) related to the changes in Earth-Sun geometry proposed by Milankovic. These intervals are referred to as Marine Isotope Stages and are counted backwards from the present day. Glacials are even numbers (MIS 2, 4, etc.) and interglacials are odd numbers (MIS 1, 3, etc.). There are three astronomical processes that ultimately regulate the amount of solar insolation received by the Earth. Precession describes the "wobble" of the axis upon which Earth

rotates (similar to the way a top spins), with a period of ~21 thousand years (kyr) (Pälike, 2003). Obliquity describes the tilt of Earth's axis of rotation with respect to the equatorial plane. The degree of tilt varies from 22-24.5 degrees, with a period of ~41 kyr (Pälike, 2003). Eccentricity describes the shape of Earth's orbit around the sun, and how that shape deviates from a perfect circle. The periodicity of variations in eccentricity are ~100 kyr and ~400 kyr (Pälike, 2003). A seminal paper by Hays et al. (1976) provides evidence that climate varies with these orbital parameters, and that these variations are recorded by oxygen isotope ratios of foraminiferal tests and faunal counts in deep-sea sediment cores.

A puzzling characteristic of the Pleistocene is the difference between the dominant orbital forcing and its climatic effect in the geologic record. It is clear that the early Pleistocene (prior to 1.2 Ma) was dominated by the relatively low amplitude 41 kyr obliquity cycle, while the late Pleistocene (~0.6 Ma − present) was dominated by the higher amplitude 100 kyr cycle (Clark et al. 2006; Figure 1). The time interval in between, the mid-Pleistocene, is known as the transition period between these two dominant variations in glaciations and deglaciations. Although the mid-Pleistocene transition (MPT) is observed in climate records such as benthic foraminiferal $\delta^{18}O$ records from ocean basins across the globe (Figure 1), the dynamics causing it are not fully understood. It is therefore of great interest in the study of Earth's geologic climate change to further our understanding of ice sheet dynamics, the hydrologic cycle, climate feedbacks, and to improve our overall ability to model such processes (Mudelsee and Schulz, 1997; Clark et al., 2006).

I hypothesize that the MPT is related to changes in oceanic heat and moisture I hypothesize that the MPT is related to changes in oceanic heat and moisture transport

as related to upper ocean hydrography in the North Atlantic Ocean. The specific hydrographic features I will be looking at are the Gulf Stream and the subtropical gyre. To test this hypothesis, I will monitor downcore changes in the coiling direction of the planktic foraminifer *Globorotalia truncatulinoides* as a proxy for reconstructing changes in the dynamics of upper ocean hydrography through time. I will construct a 0.8 million-year record of down-core changes in the coiling direction of *G. truncatulinoides* using sediments from Ocean Drilling Program (ODP) Site 1058 in the northwestern subtropical Atlantic Ocean (Figure 2). Since my site is located near the Gulf Stream, the sediments I am analyzing should represent changes in the relative strength and position of the Gulf Stream, which is the western boundary of the North Atlantic subtropical gyre. Variations in the coiling ratio of *G. truncatulinoides* are indicative of changes in the hydrography of the study region (Ufkes and Kroon, 2012; Feldmeijer et al., 2014; Billups et al., 2016); I will attempt to relate these changes to changes in poleward warm water transport cross the mid-Pleistocene transition. By comparing my record to coiling ratio data from other sites in the North Atlantic, I will be able to reconstruct the upper ocean hydrography of this region and relate this to large-scale changes in ocean circulation across the study interval. Understanding the hydrography of this region is fundamental in characterizing and understanding climate change across the MPT due to the relationship between global ocean circulation, the atmosphere, and ice-sheet dynamics.
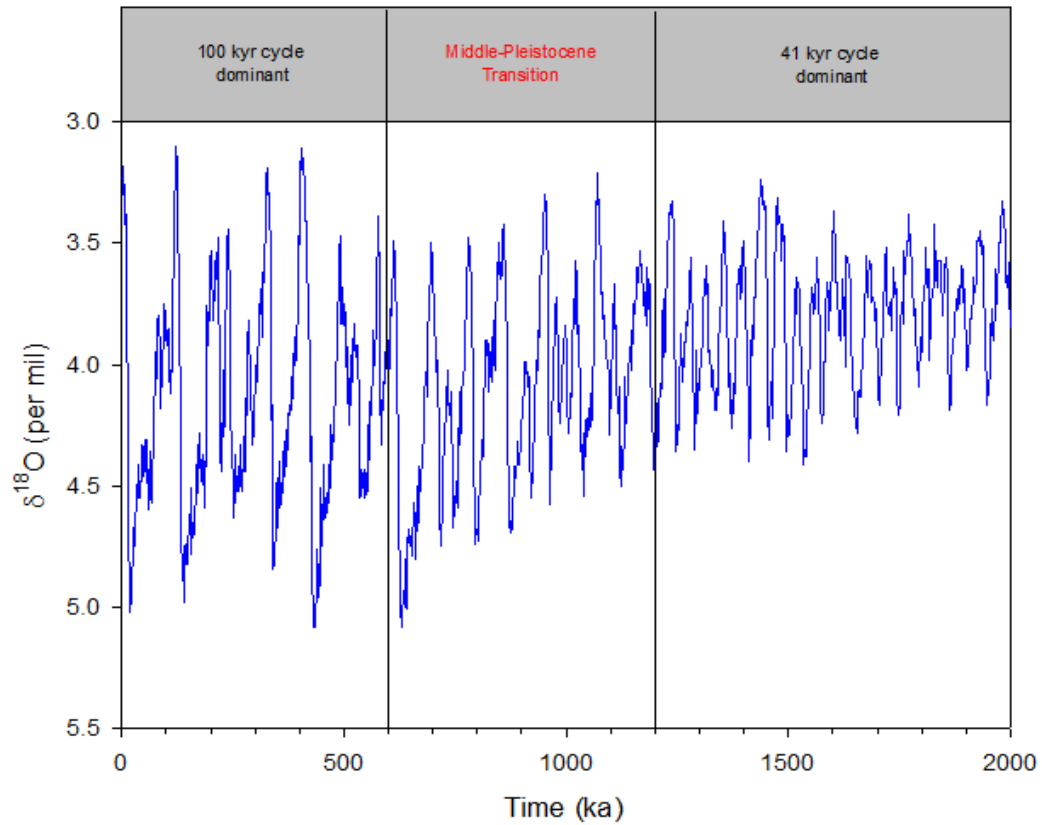
Figure 1.   Climate record using $\delta^{18}O$ measurements from benthic foraminifera (from Lisiecki and Raymo, 2005). The oxygen isotope record is produced by the fractionation of oxygen isotopes during evaporation and precipitation. More positive $\delta^{18}O$ values indicate more ice on land and/or a cooling of deep-ocean temperatures (glacial periods), whereas more negative $\delta^{18}O$ values indicate smaller or non-existent ice sheets and/or a warming of deep-ocean temperatures (interglacial periods). Time is presented in thousands of years age (ka), where 0 ka is the present day.
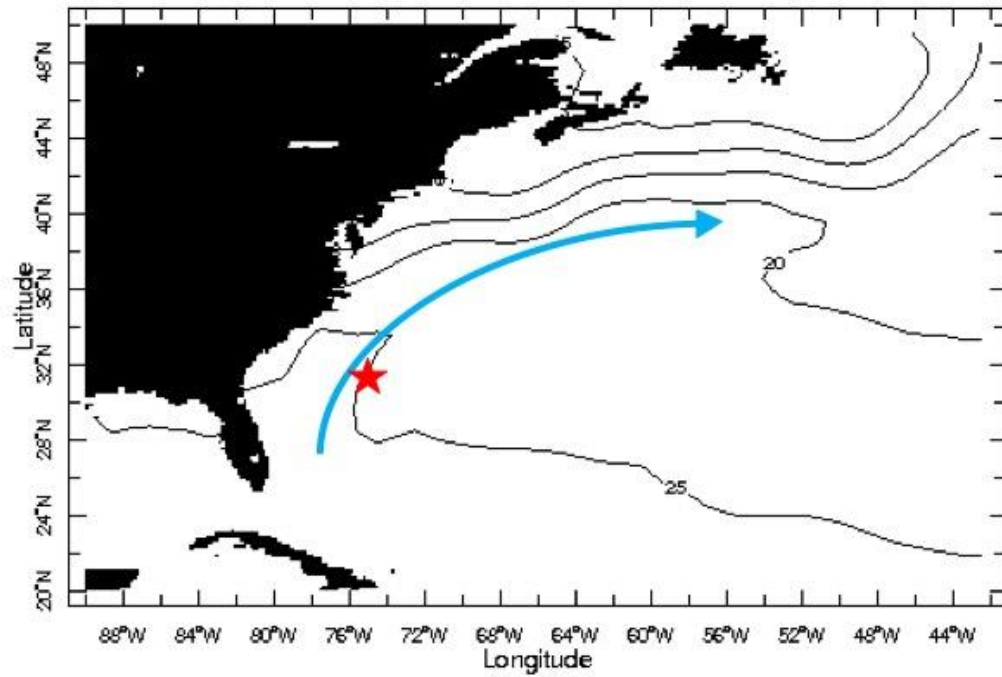
May 2017

Figure 2.   North Atlantic sea surface temperature in May 2017 (Reynolds et al., 2002). Red star indicates the location of the study site near the Gulf Stream (approximated by the blue arrow). Figure was generated using the interactive website of the Lamont Doherty Earth Observatory.

Chapter 2

BACKGROUND

2.1   Mid-Pleistocene Transition

The defining characteristic of the MPT is the increase in severity of glaciations corresponding to the onset of the 100 kyr cycle which began around 1 Ma. This is clearly observed in the $\delta^{18}O$ record through an increase in amplitude (i.e., severity) and a decrease in frequency (compared to the pre-MPT) of the global $\delta^{18}O$ signal (Lisiecki and Raymo, 2005; Clark et al., 2006). Clark et al. (2006) also state that the dominant 100 kyr cycle, which was fully established approximately 600 ka, is defined by the maximum glaciations we know occurred at that time. Although the dominant cycle controlling ice-volume over the last 600 kyr has been the 100 kyr cycle, there is no corresponding signal in solar insolation; therefore, any proposed mechanisms for the cause of the MPT should also include a reason that the 100 kyr cycle was prevented from being dominant prior to 1.2 Ma (Clark et al. 2006).

The absence of a direct relationship between solar insolation forcing and glacial-interglacial cyclicity has generated a general agreement that there was a response of the climate system during the MPT (Hays et al., 1976; Petit et al., 1999; Lisiecki and Raymo, 2005; Clark et al., 2006). A primary focus of the climate system, particularly across glacial-interglacial intervals, is ice sheet dynamics. Some of the major factors in the growth and decay of ice sheets include the time required to grow and melt an ice sheet, the rates of accumulation and ablation (loss of snow or ice) over the ice sheet, and the relationships between these four factors (Weertman, 1964). For

example, Weertman (1964) showed that the time required to melt an ice sheet is less than the time it takes for an ice sheet to grow, assuming that ablation rates are greater than accumulation rates. This brings forth the concept that the growth of an ice sheet may trigger its own decay, which provided early evidence for the ice-age theory (Weertman, 1964). Additionally, the amount of solar insolation received interacts with a threshold temperature for ice sheet growth (Ruddiman, 2008). If the maximum amount of solar insolation is below this threshold, continents were too warm for ice sheets to grow. When the maximum amount of solar insolation crossed the threshold, ice sheets could grow larger and persist for longer periods of time. Clark and Pollard (1998), modelling ice sheet dynamics and bedrock deformation over the last 3 Ma, argued that the change in amplitude and timing of glaciations during the MPT was due to a change in the type of sediment underneath the ice sheet. Prior to the MPT, the sediments underneath the Laurentide ice sheet were soft and easily deformable, causing the ice sheet to remain relatively thin and respond to the dominant 41 kyr orbital forcing; continual erosion of this sediment layer throughout the MPT revealed a harder, deeper bedrock surface, which allowed the ice sheet to grow thicker and respond to glaciations on the 100 kyr timescales that characterize glaciations and deglaciations of recent times (Clark and Pollard, 1998). Other responses of the climate system during the growth and decay of ice sheets include local conditions specific to the location of ice sheets, the effect of albedo feedback on global surface temperature, the relationship between elevation and ice accumulation, as well as processes that destabilize ice sheets, and are discussed in depth by Oerlemans (1991).

There have been many other studies offering additional explanations for this response of the climate system during this transition period. Berger et al. (1999) used a

model to simulate the response of Northern Hemisphere ice sheet volume to differing atmospheric CO_2 concentrations. When applying a decreasing CO_2 concentration over the last 3 million years, their model simulated the 100-kyr cycle being dominant only in the last 1 Myr, while the 41-kyr cycle was dominant before that. Although these results are similar to the $\delta^{18}O$ data observed in the geologic record, the authors stress that their model contains simplified impacts from clouds, water vapor and albedo, and does not consider processes impacting CO_2 concentrations aside from the atmosphere, namely oceanic and anthropogenic (Berger et al., 1999). Tziperman and Gildor (2003) proposed that the MPT was triggered by long-term deep-water cooling. The accompanying climate response was what they termed the sea ice switch mechanism of glacial cycles. Sea ice has the ability to "switch" the climate system from a mode of glaciation to a mode of deglaciation due to its rapid growth and melting and its effect on energy balance, ice sheet mass balance, and air-sea fluxes. The authors do not specify the cause of deep-water cooling or any other ocean dynamics aside from temperature, instead focusing on how that cooling caused their sea ice switch mechanism to control ice volume (Tziperman and Gildor, 2003).

2.2   Foraminifera

Foraminifera are microscopic zooplankton that build shells, or tests, out of calcium carbonate ($CaCO_3$) (Bé, A.W.H., 1977). The process of calcification in foraminifera and many other marine organisms is well understood, and described by the following equation (Balch et al., 1991; Barker and Elderfield, 2002):

$$Ca^{2+} + 2HCO_3^- \rightarrow CaCO_3 + CO_2 + H_2O$$

There are two classifications of foraminifera based on where they live in the marine environment. Benthic species live on or within the seafloor, and planktic species live suspended in the water column. While benthic species are the most diverse, planktic species are the most abundant. The tests of foraminifera are a defining characteristic of these organisms. They are segmented or chambered with a prominent opening in one end. The carbon and oxygen used to build their tests comes from bicarbonate (HCO_3^-) ions in seawater – for this reason, the geochemistry of the tests of these organisms can be used to provide information about the environmental conditions of the geologic past (Bé, A.W.H., 1977; Healy-Williams, 1983; Lohmann and Schweitzer, 1990). This proxy is very robust and has become a very popular tool for the paleoclimatologist and paleoceanographer.

Globorotalia truncatulinoides is a deep-dwelling species that has been found to reproduce at ~600m and calcify as deep as ~1000m (Lohmann and Schweitzer, 1990; Feldmeijer et al., 2014). This species has been used as a paleoceanographic indicator for decades (Ericson et al., 1954; Bé et al., 1971; Thiede, 1971; Herman, 1972; Lohmann and Malmgren, 1983; Lohmann and Schweitzer, 1990; Lohmann, 1992; Matsumoto and Lynch-Stieglitz, 2003; Renaud and Schmidt, 2003; LeGrande et al., 2004; Cléroux et al., 2009; Feldmeijer et al., 2014; Billups et al., 2016). A unique characteristic of this species is that their tests exhibit dimorphism, meaning that within this species, individual tests can have different morphologies (de Vargas et al., 2001; Ujiié et al., 2010). The coiling direction of the test is either clockwise (dextral, to the right; Figure 3c and 3d) or counterclockwise (sinistral, to the left; Figure 3a and 3b) when viewed from the ventral side. Coiling directions have been known to change over glacial-interglacial time periods; while traditionally associated with

environmental or geographic factors (Ericson et al., 1954; Hemleben et al., 1989), changes in coiling direction have recently been associated with genetic variations within this species (Ujiié et al., 2010). Therefore, coiling ratios of *G. truncatulinoides* in deep-sea sediments are extremely useful proxies used in paleoceanographic studies to reconstruct upper ocean hydrography.

The coiling direction of *G. truncatulinoides* has been related to depth habitat, water masses, and seasonal changes in temperature, salinity, and mixing (Ericson et al., 1954; Bé, 1960; Herman, 1972; Lohmann, 1992), and has been used to reconstruct past changes in the depth of the permanent thermocline (Feldmijer et al., 2014), which all have implications in evaluating heat distribution within the ocean. Feldmeijer et al. (2014) found that changes in the dominant coiling ratio through time suggests periods when the permanent thermocline deepened or shallowed and related these changes in the depth of the thermocline to large scale ice rafting events during the transitions from glacials to interglacials, as well as detailed the subsequent effect of these freshwater inputs on Atlantic meridional overturning circulation during the time interval studied. Billups et al. (2016), analyzing sediments from ODP Site 1059 in the subtropical northwestern Atlantic Ocean, observed a general pattern of sinistral *G. truncatulinoides* dominance during interglacial periods, while glacial periods were characterized by lower abundances or even absences of the left-coiling variety. Since this data comes from the same study region, the results are extremely pertinent to my research. The results of this and other studies (Ericson et al., 1954; Ujiié et al., 2010) support my expectations to observe sinistral *G. truncatulinoides* dominance during interglacials due to the influence of waters from the subtropical gyre.

Additionally, the oxygen isotope composition of the tests of *G. truncatulinoides* has been used to estimate calcification depths and depth habitat of the organisms, providing an extra method for reconstructing upper ocean hydrography (Cléroux et al., 2007; Cléroux et al., 2009; LeGrande et al., 2004). This is possible through knowledge of the life cycle of *G. truncatulinoides* and its association between water column structure, including upwelling and vertical mixing (Lohmann and Schweitzer, 1990). While oxygen isotope ratios provide paleoceanographers with an additional method to produce reconstructions of the oceans, the data have not been found to correlate with coiling ratios of *G. truncatulinoides* (Feldmeijer et al., 2014).

2.3   Ocean Circulation and Reconstruction

The Gulf Stream is the western boundary current of the North Atlantic subtropical gyre. It travels northward up the east coast of North America and across the North Atlantic, transporting a tremendous amount of water (up to 150 Sverdrups at its maximum); therefore, this current, and its extension, the North Atlantic Current, transports a large amount of heat from the equatorial North Atlantic to the polar North Atlantic (Schmitz and McCartney, 1993). This heat transport is highly influential in moderating North Atlantic climate, so changes in the flow of this current may impact climate change on larger temporal and spatial scales (Seager et al., 2002; Lund et al., 2006).

In fact, Broecker et al. (1985) and Carlson et al. (2008), for example, have shown that changes in Gulf Stream dynamics are associated with changes in global thermohaline circulation (Figure 4). As this water travels to mid-latitudes, it experiences a great deal of evaporation, increasing its salinity. As this saline water travels to higher latitudes, it cools, becoming very dense, and sinks in the North

11

Atlantic and Nordic Seas (Schmitz and McCartney, 1993). This is the formation of North Atlantic Deep Water (NADW) and is a driving factor in the overturning of North Atlantic waters, which we refer to as thermohaline circulation. Freshening of North Atlantic waters in the geologic past has caused reductions in the strength of the overturning circulation, subsequently influencing global climate (Carlson et al., 2008). This system is therefore very dynamic and sensitive to change.

The ability to track changes in and reconstruct ocean circulation over glacial-interglacial timescales is possible through the use of carbon isotope ratios, specifically the $\delta^{13}C$ ratio of benthic foraminifera (Oppo and Fairbanks, 1987; Raymo et al., 1989; Raymo et al., 1990; Raymo et al., 1997). Water masses have a particular $\delta^{13}C$ signature, which is associated with the fractionation of carbon isotopes and the forms of dissolved carbon of the source of the water mass (Kroopnick, 1985). When water masses mix as they travel around the globe, the $\delta^{13}C$ signature changes, depending on the value of each water mass and the specific water masses being mixed (Oppo and Fairbanks, 1987). The $\delta^{13}C$ signature incorporated into the tests of foraminifera represents the carbon isotope ratio of the water mass in which they calcify. Down-core changes in benthic foraminiferal $\delta^{13}C$ values are used to show the relationship between water masses of different origins, and how these relationships and dynamics of the water masses change and subsequently influence climate through time.

Examples of this paleo-deepwater reconstruction technique come from many different studies that compare $\delta^{13}C$ values of benthic foraminifera to trace the movement of deepwater masses over glacial-interglacial timescales. Oppo and Fairbanks (1987) examined records spanning the Last Glacial Maximum, studying the contribution of NADW to Southern Ocean water and showing the connection between

12

deep water masses of opposite hemispheres associated with climate. Raymo et al. (1997) examined δ^{13}C records from sites in the North Atlantic to reconstruct thermohaline circulation and deep-ocean chemistry during an interval spanning the mid-Pleistocene climate transition. Poirer and Billups (2014) analyzed benthic foraminiferal carbon isotope ratios across the mid-Pleistocene, finding low δ^{13}C values during glacial extremes and high δ^{13}C values during interglacial periods. These higher values of δ^{13}C imply stronger, northern-sourced deepwater formation during the MPT, which is similar to modern circulation. Lear et al. (2016) analyzed benthic foraminiferal stable isotope records in relation to trace metal records, finding changes in nutrient content and carbon saturation state of ocean waters during the MPT. Their findings imply changes in the ocean's ability to store carbon and changes in air-sea CO_2 exchange, where decreases in δ^{13}C values resulted in increased deep ocean carbon storage and reduced atmospheric pCO_2.

One study examining the dynamics of the MPT that is most relevant to my research comes from Pena and Goldstein (2014). Using neodymium isotopes to trace North Atlantic Deep Water export to the Southern Ocean, the authors recorded a major change in the ocean's thermohaline circulation during the MPT. They concluded that prior to the MPT, there was relatively little variability in the contribution of North Atlantic sourced waters to the Southern Ocean between glacials and interglacials. The post-MPT period is characterized by strong thermohaline circulation during interglacials, similar to the pre-MPT period. During glacial periods, however, this contribution of North Atlantic water, and therefore the strength of the ocean's thermohaline circulation, was much weaker. The authors state that this first occurrence of disrupted ocean circulation (approximately 950-860 ka) is essentially the initiation

of the first 100-kyr glacial cycle (Pena and Goldstein, 2014). The combination of this weakening and other feedback mechanisms, such as the size of North Atlantic ice sheets, atmospheric CO_2 drawdown, ocean cooling, and low Southern Hemisphere summer insolation, during this first 100-kyr cycle led to long-lasting increases in the duration of glacial-interglacial cycles as well as the intensity of glacials, which are notable characteristics of the MPT and the current glacial cycle (Pena and Goldstein 2014).

The evidence of changes in ocean circulation across the MPT from this study are relevant to my research because my samples come from an area of the North Atlantic that has implications as a surface limb of thermohaline circulation on glacial-interglacial timescales. This will allow me to relate changes in coiling direction to large-scale ocean circulation events across the MPT, specifically, the ending of the 41-kyr world and the establishment of the 100-kyr world. In order to track these changes through time, I will compare my coiling ratio data to $\delta^{18}O$ records to represent the background climate during my study interval. By comparing my record to other coiling ratio records from sites in the North Atlantic along the same path of circulation, I will establish spatial patterns in the North Atlantic surface ocean. I will then attempt to correlate my coiling ratio data to the current knowledge of deepwater circulation throughout the MPT. This will be a valuable contribution to further analyze characteristics and dynamics of ocean circulation during the MPT.

Figure 3.   Microscope picture of sinistral *G. truncatulinoides* (A and B) and dextral
              G. truncatulinoides (C and D). A and C are views from the dorsal side; B
              and D are views from the ventral side.
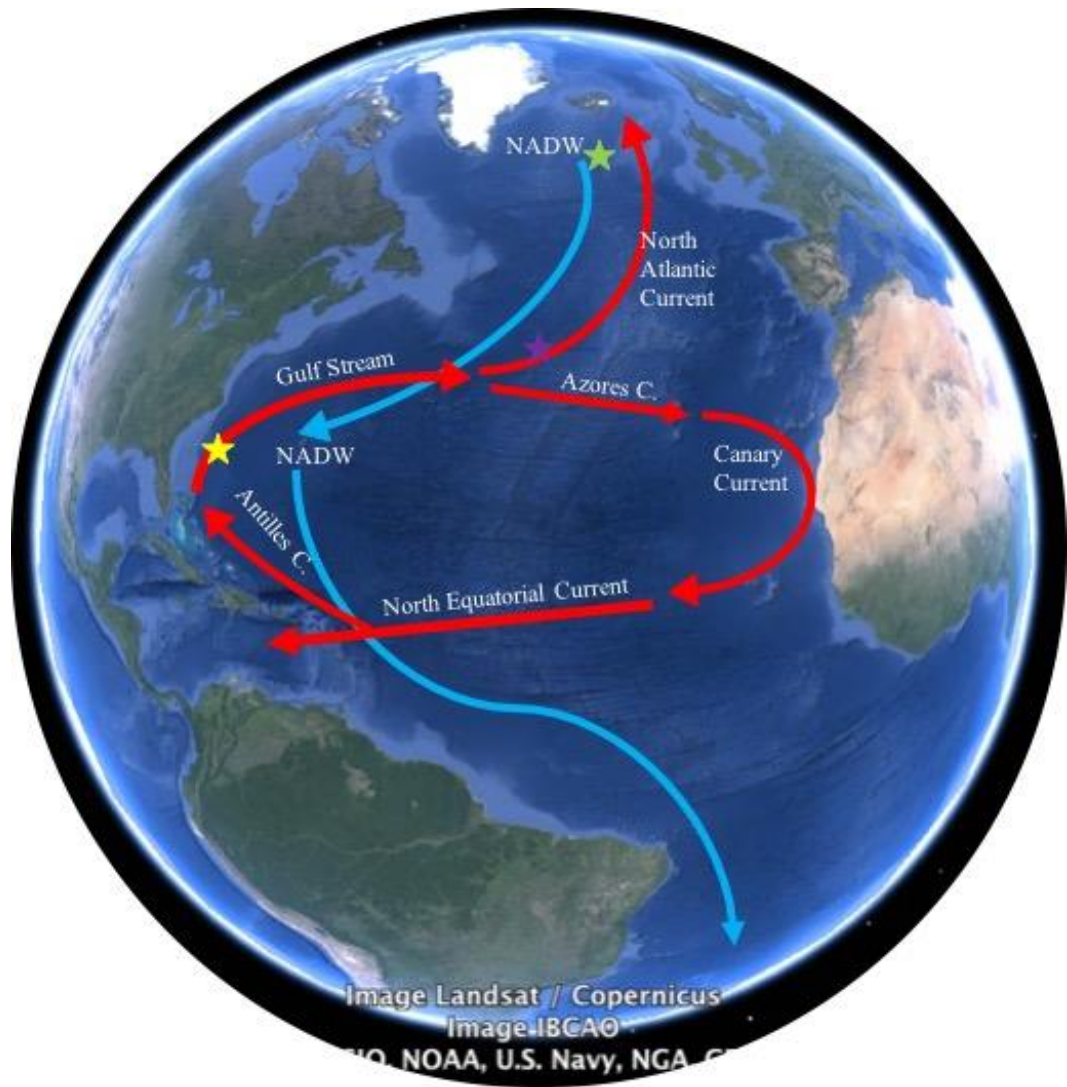
Figure 4.   A general schematic of ocean circulation in the North Atlantic. Warm, surface currents are represented by red arrows. Cold, deep-water currents are represented by blue arrows. The study site (Site 1058) is identified by the yellow star. The sites used for comparison are Site 607 (purple star) and Site 552 (green star).

Chapter 3

RESEARCH STRATEGY

3.1 Study Site 1058

ODP Site 1058 (31°N, 75°W) is located on the Blake Bahama Outer Ridge at
~2,984m water depth in the northwestern subtropical Atlantic Ocean. Site 1058 lies
near the modern Gulf Stream and within the path of the flow of lower NADW to the
South Atlantic (Figure 4). Sedimentation at this site is related to the sensitivity of these
currents over glacial-interglacial timescales (Keigwin et al., 1998). Additionally, Site
1058 lies on the border of the distribution zone of left and right coiling species of *G.
truncatulinoides* (Ericson et al., 1954; Ujiié 2010). Consequently, the change in
dominant coiling direction through time should represent the movement of the Gulf
Stream and the subtropical gyre with respect to this location. Therefore, Site 1058 is
an ideal location to study changes in the upper ocean hydrography of the subtropical
North Atlantic in the geologic past.

3.2 Use of *Globorotalia truncatulinoides*

Prior work has shown that the left-coiling variety of *G. truncatulinoides* is
indicative of influence of waters from the center of the North Atlantic subtropical
gyre, whereas dominance of the right-coiling species is indicative of influence of
waters from the gyre margins (Renaud and Schmidt, 2003). While this proxy cannot
reconstruct the precise location or strength of the paleo-Gulf Stream, it allows
inferences to be made about the relative position of the Gulf Stream with respect to the

study site based on the dominance of one coiling direction over the other. As changes in the coiling ratio of *G. truncatulinoides* represent changes in the hydrography of the study region, this proxy provides a method to reconstruct the relative position of the Gulf Stream, and thus the hydrography of the North Atlantic subtropical gyre, through time. My goal was to relate these changes in hydrography throughout the North Atlantic to large-scale surface ocean circulation, and ultimately to explore the influence of heat transport across the mid-Pleistocene transition.

3.3   Study Interval and Temporal Resolution

The study interval for my research is 0.4 Ma – 1.2 Ma. This time interval comprises the mid-Pleistocene transition (Figure 1). Prior to 1.2 Ma, cycles of glaciation and deglaciation were relatively weaker and more frequent, following the 41 kyr obliquity-paced cycle. Since ~0.6 Ma, the intensity of glacial cycles has increased and has followed 100 kyr cycles. This interval of time is appropriate to study the dynamics of the mid-Pleistocene transition because it is long enough to encompass both the end of the 41 kyr "world" (Raymo and Nisancioglu, 2003) and the firm establishment of the 100 kyr cycle. To resolve and observe the evolution of these orbital cycles in my record, I sampled at 20-40 cm intervals, which results in a time step of ~2000-4000 years.

3.4   Sediments and Sampling

Two distinct lithological units were observed at Site 1058. Unit 1 (Holocene to mid-Pleistocene) is defined by higher carbonate content and color variability than unit 2 (mid-Pleistocene to early Pleistocene), with both units containing alternating layers of nannofossil-rich sediments and clay-dominated sediments (Keigwin et al., 1998).

The transition from Unit 2 to Unit 1 (deepest, and therefore oldest sediments to shallowest, and therefore youngest sediments) is representative of the transition from 41-kyr to 100-kyr climate variability; the alternating layers of nannofossil ooze and clays within units reflects interglacial and glacial periods, respectively (Keigwin et al., 1998).

Sedimentation rates and age-depth relationships were determined by biostratigraphic datums and magnetostratigraphy, with the oldest sediments recovered dating to the early Pleistocene (Keigwin et al., 1998). The combination of relatively high sedimentation rates, age-depth model (Figure 5; Weirauch et al., 2008), and overall core recovery affirm that sediments from this site are continuous and represent time from the early Pleistocene to the Holocene. The age-depth model constructed for sediments at Site 1058 was produced using data from Weirauch et al. (2008). Since this model was tuned using a planktic foraminiferal $\delta^{18}O$ from this site, it is appropriate for me to use it in my research.

3.5   Comparison to North Atlantic Sites

In order to reconstruct surface ocean circulation in the North Atlantic, I compared the coiling ratio of *G. truncatulinoides* at Site 1058 to the coiling ratio at other sites in the North Atlantic (Kaiser et al., 2018). These sites lie along the same path of circulation as Site 1058 and represent different sections of the North Atlantic subtropical gyre (Figure 4); this comparison will therefore establish a link between surface ocean circulation from the lower to the higher latitudes.

Site 607 (41°N, 32°W) is located at the northernmost part of the subtropical gyre, representing the Northern gyre margin (Ruddiman, Sarnthein et al., 1988). This site should be a good representation of the middle latitudes in the North Atlantic due

to the hydrography of this area of the North Atlantic. It is located where the Gulf Stream turns northward into the North Atlantic Current (Figure 4) and should therefore be influenced by changes in the hydrography of the subtropical gyre.

Site 552 (56°N, 23°W) is the poleward-most site in this study, representing the high-latitude reach of the North Atlantic Current (Roberts, Schnitker et al., 1984; Schmitz and McCartney, 1993). It is located where warm, salty waters from the subtropical North Atlantic turn northward to be transported to the polar North Atlantic by the North Atlantic Current; these waters then cool and sink to form North Atlantic Deep Water (Figure 4). This site provides a good representation of the subpolar North Atlantic with the potential to observe changes in surface to intermediate water convection.

Comparing the coiling ratio of *G. truncatulinoides* at these three sites provides a spatial representation of the data and shows how consistent these observations are on this spatial scale in the North Atlantic across the mid-Pleistocene transition. The locations of these three sites represents a latitudinal gradient that spans the subtropical to the subpolar North Atlantic. Therefore, any record of oceanographic changes at one site should be present in the others.

3.6   Age Model

The age model for Site 1058 is based on foraminiferal oxygen isotope stratigraphy. Oxygen isotope stratigraphy is the concept that variations in oxygen isotope ratios ($\delta^{18}O$) measured in carbonates are globally synchronous because they represent the growth and decay of ice sheets and the relationship with the hydrologic cycle caused by orbital forcings (obliquity and precession) (Shackleton, 1967; Berger

et al., 1984; Jansen, 1989; Lisiecki and Raymo, 2005). Therefore, the $\delta^{18}O$ record represents background glacial-interglacial climate change at the sites in this study.

More specifically, this approach is possible due to the process of isotope fractionation and its relationship with temperature. There are two main isotopes of oxygen: ^{16}O (8 protons and 8 neutrons) and ^{18}O (8 protons and 10 neutrons). This discrepancy in the number of neutrons is enough to cause ^{16}O to be relatively lighter than ^{18}O. This mass difference has an influence on the transport of each isotope. In the equatorial oceans, as evaporation occurs, the lighter ^{16}O evaporates more readily than the heavier ^{18}O. Therefore, at these latitudes, seawater is relatively enriched in ^{18}O (or depleted in ^{16}O), whereas water vapor is relatively depleted in ^{18}O (or enriched in ^{16}O). As water vapor travels poleward through the mid latitudes, precipitation occurs. Opposite of evaporation, the heavier ^{18}O preferentially condenses and rains/snows out more readily than the lighter ^{16}O. This fractionation process continues to enrich seawater in ^{18}O and enrich water vapor in ^{16}O. By the time atmospheric water vapor reaches the poles, it is very enriched in ^{16}O relative to when it formed at the equator. Therefore, the ice sheets formed by precipitating snow are enriched in ^{16}O. The ratio of oxygen isotopes in a sample are compared to an international standard and reported as per mil, meaning parts per thousand (Emiliani, 1955).

Following these changes in oxygen isotope ratios through time allows for the interpretation of climate change over glacial-interglacial time scales. As ice sheets grow during a glaciation, more ^{16}O gets removed from the ocean and locked away on land. This causes the ocean to be very enriched in ^{18}O. Conversely, during an interglacial period, the ice sheets melt, returning freshwater rich in ^{16}O back into the ocean. Organisms that build calcium carbonate shells take up the oxygen in the

seawater. When these organisms die, their shells sink to the seafloor and get buried by sediments, preserving the oxygen isotope ratio of the water in which their shell was built. Shells formed in cold, glacial environments would have a higher ^{18}O content relative to the oceans during a warm interglacial period.

Since one of my primary objectives is to compare the coiling ratio of *G. truncatulinoides* at Site 1058 to other sites in the North Atlantic, it is crucial that the $\delta^{18}O$ records and age models from the other sites are comparable to Site 1058. Since ice volume is a global signal and the age models for the other sites are also based on oxygen isotope stratigraphy (Roberts, Schnitker, et al., 1984; Ruddiman, Sarnthein, et al., 1988; Grüetzner et al., 2002), it can be assumed that there is agreement between the three sites, and changes between sites are concurrent. This is clearly represented in Figure 6, where the $\delta^{18}O$ records from each site are compared. Heavier values of $\delta^{18}O$ (representing glacials) and lighter values of $\delta^{18}O$ (representing interglacials) occur at the same time at all sites.
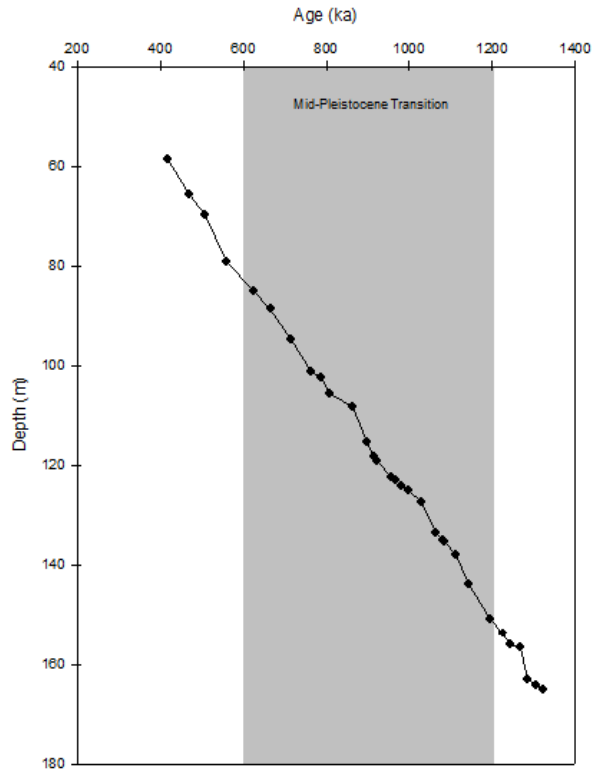
Figure 5.   Age-Depth Model. Control points were determined by tuning the planktic foraminiferal δ¹⁸O record to Northern Hemisphere summer insolation. Data from Weirauch et al. (2008).
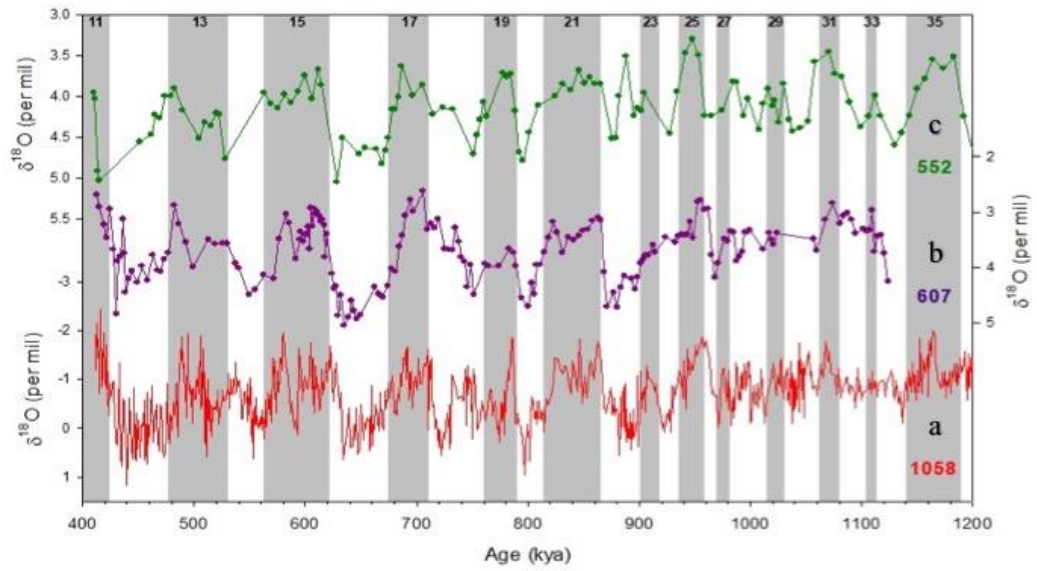
Figure 6.   Foraminiferal δ18O records for sites with *G. truncatulinoides* coiling ratio data used in this study. Sites 607 (purple) and 552 (green) record benthic δ18O records. Site 1058 (red) records the planktonic foraminifer *Globigerinoides ruber* δ18O record.

Chapter 4

METHODS

The *G. truncatulinoides* time series being collected for this research came from approximately 350 samples from archived ODP cores from Site 1058, spanning ~0.4 Ma to 1.2 Ma. All samples were washed, dried, and size fractioned to >150 microns (μm). Before picking, each sample was sub-sieved at the 355 μm size fraction to include adult specimens of *G. truncatulinoides* (Ujiié et al. 2010). Feldmeijer et al. (2014) found that when analyzing smaller size fractions, changes in coiling direction are constant – I therefore assumed that the 355 μm size fraction was sufficient for my counts.

After size fractioning, the process of picking began by sprinkling the sample evenly across a picking tray. Tests were picked under a binocular microscope using the tip of a very fine artist's brush. Left and right coiling tests were separated and placed on a microfossil slide, then counted for calculating the ratio of left : right coiling tests.

The percentage of sinistral *G. truncatulinoides* tests for each sample was calculated by the following equation and was be reported as variations downcore (i.e., through time).

$$\left(\frac{G.truncatulinoides_{sinistral} \text{ counts}}{G.truncatulinoides_{sinistral} \text{ counts} + G.truncatulinoides_{dextral} \text{ counts}} \right) * 100$$

This ratio is appropriate for this study because it is independent of other components of sediment samples, such as grain size or carbonates. I compared the

percent sinistral *G. truncatulinoides* data with the published *G. ruber* $\delta^{18}O$ record from this site (Weirauch et al., 2008). The $\delta^{18}O$ record represents the background glacial-interglacial climate change during my time interval. This allowed me to make inferences about the relationship between change in coiling direction and climate changes over glacial-interglacial timescales.

Chapter 5

RESULTS

5.1 Coiling Ratios in the subtropical Northwestern Atlantic Ocean

Core-top and the uppermost sediments from Site 1058 representing the most recent interglacial MIS 1 (the Holocene) are dominated by sinistral *G. truncatulinoides* (Figure 7). The samples are in the range of 74-86% sinistral with an average percentage of 79%, consistent with the distribution pattern observed by Ericson et al. (1954) and Ujiié et al. (2010).

The sediment record at Site 1058 indicates variations in the downcore abundance of total *G. truncatulinoides* tests throughout the study interval (400-1200 kya). The site records a general long-term trend of extended periods primarily dominated by dextral *G. truncatulinoides* (generally at least 50%) with variation in the proportion of sinistral *G. truncatulinoides* (observations range from 0-50%). MIS 35-37 (~1160-1220 kya), MIS 22-32 (~880-1100 kya), and MIS 15-21 (~600-850) all are intervals where dextral *G. truncatulinoides* is the dominant variety, although the intermittent presence of sinistral *G. truncatulinoides* occasionally reaches upwards of 40% (Figure 8). These intervals of little to no presence of sinistral *G. truncatulinoides* are so long that it is not possible to distinguish any relationship with the glacial-interglacial climate background.

Throughout the study interval, there are occasional intervals dominated by sinistral *G. truncatulinoides* (>50%) with abundances similar to or greater than the late Holocene (~80%). Interglacial MIS 35 (~1140 kya), MIS 33 (~1110 kya), MIS 21

(~865 kya), MIS 15 (~575 kya), MIS 13 (~530 and ~480 kya), and MIS 11 (~420 kya), and glacial MIS 34 (~1120 kya), MIS 22 (~870 kya), MIS 14 (~545 kya), and MIS 12 (~430 kya) all record maxima in sinistral *G. truncatulinoides* (Figure 8). Additionally, throughout the study interval, multiple peaks were recorded within one marine isotope stage (MIS 22, 14, 13, and 12). During these time periods, there is too much variation to distinguish a relationship with the glacial-interglacial climate background.

Several trends in the coiling ratio are apparent in the time periods prior to and before the midpoint of the mid-Pleistocene transition centered around 900 kya. The pre-MPT interval (MIS 22-32, ~880-1100 kya) is dominated by dextral *G. truncatulinoides*, although there are frequent and somewhat periodic occurrences of sinistral *G. truncatulinoides* (Figure 8). The beginning of the post-MPT interval (MIS 15-21, ~600-850) is dominated by dextral *G. truncatulinoides*, with little to no appearance of sinistral *G. truncatulinoides* for ~200 kyr (Figure 8). From ~600-400 kya, Site 1058 records multiple distinct peaks in sinistral *G. truncatulinoides* that reach levels as high as pre-MPT and occur more frequently in comparison (Figure 8). The midpoint of the MPT (MIS 22/21, ~870 kya) is recorded by an ~20 kyr long interval of sinistral *G. truncatulinoides* dominance (Figure 8). Overall, there is no clear relationship between the dominant coiling variety and the glacial-interglacial background climate; in fact, variations in the coiling direction of *G. truncatulinoides* at Site 1058 appear to be more frequent than the background climate.

5.2 Coiling Ratios at Other Sites in the North Atlantic

Other sites in the North Atlantic also show a similar long-term trend of long periods dominated by dextral *G. truncatulinoides* interspersed with occurrences of

sinistral *G. truncatulinoides*, as well as occasional intervals dominated by sinistral *G. truncatulinoides* (Figure 9). At Site 607, similar to Site 1058, there is no clear relationship between the dominant coiling variety and the glacial-interglacial background climate. Interglacial MIS 31 (~1065 kya), MIS 21 (~865 kya), MIS 13 (~530 kya), and and MIS 11 (~415 kya), and glacial MIS 32 (~1090 kya), MIS 26 (~970 kya), MIS 24 (~930 kya), MIS 14 (~550 kya), and MIS 12 (~430 kya), all record maxima (>50%) in sinistral *G. truncatulinoides* at Site 607. The pre-MPT coiling ratio data at this site is characterized by much greater variability in the presence of sinistral *G. truncatulinoides* compared to Site 1058 (Figure 9b). However, the post-MPT interval at this site records primarily dextral *G. truncatulinoides* dominance (similar to Site 1058) with noticeably fewer and less pronounced occurrences of sinistral *G. truncatulinoides* compared to the pre-MPT interval (Figure 9b). While some of the sinistral maxima at Site 607 occur at the same time as maxima at Site 1058 (MIS 22/21, 14, 13, and 11), other maxima at Site 607 occur when there is a disappearance of sinistral *G. truncatulinoides* at Site 1058 (MIS 32, 31, and 24).

At the high-latitude Site 552 (Figure 6c), the abundance of *G. truncatulinoides* was relatively low. *G. truncatulinoides* is primarily a subtropical species but has also been observed in subpolar waters; however, its abundance tends to decrease with increasing latitude (Tolderlund and Bé, 1971). On average, samples from Site 552 contained 14 tests, compared to 127 at Site 607 and 69 at Site 1058. To account for discrepancy in abundance, only samples containing at least 20 individual tests were considered when determining maxima in sinistral *G. truncatulinoides*. This resulted in fewer, but considerably more robust data points at this site relative to the raw data. Unlike Sites 1058 and 607, the maxima in sinistral *G. truncatulinoides* at Site 552 tend

to occur during interglacial periods (MIS 21, ~860 kya; MIS 15, ~580 kya; MIS 13, ~530 kya and ~480 kya) (Figure 6c). Aside from these maxima, the majority of this record is dominated by dextral *G. truncatulinoides* whether looking at pre or post-MPT (Figure 6c). Although there are fewer maxima at Site 552 (due to fewer data points), the observed maxima occur at roughly the same time as maxima at Site 1058 and 607 (MIS 22, 15, and 13). The greatest number of tests were counted at MIS 21 (856 kya, 91 tests; 860 kya, 50 tests; 863 kya, 47 tests), MIS 22 (866 kya, 41 tests), and MIS 13 (480 kya, 48 tests). The majority of samples considered robust at Site 552 contained between 20-40 tests. It is worth noting that since samples with less than 20 tests were not considered at Site 552, some maxima in sinistral *G. truncatulinoides* at Sites 1058 and 607 are not observed at Site 552.

Across the mid-point of the MPT (the interval MIS 23-21), there is a pattern in sinistral *G. truncatulinoides* dominance from one site to the next. Through MIS 23, all three sites record dominance of dextral *G. truncatulinoides*. During the beginning of MIS 22, Sites 1058 and 552 continue to be dominated by dextral *G. truncatulinoides*, while Site 607 begins to record the presence of sinistral *G. truncatulinoides* upwards of 40%. Towards the end of MIS 22 (~880 kya), Site 1058 records a massive change in the dominant coiling ratio, with sinistral *G. truncatulinoides* presence in the range of 80-100%. This shift in dominance occurs first at Site 1058, then slightly later at Site 607, and finally at Site 552 as interglacial MIS 21 begins. This trend very quickly (by ~860 kya) returns to dextral *G. truncatulinoides* dominance at all three sites.

To summarize, the core-top data from Site 1058 shows the expected distribution pattern from Ujiié et al. (2010), confirming that sinistral *G. truncatulinoides* are the dominant species in this region of the subtropical North

Atlantic during the most recent interglacial MIS 1. When comparing similarities between the three sites, there are three features that stand out the most: (1) All sites record a significant peak in sinistral *G. truncatulinoides* dominance during the midpoint of the mid-Pleistocene transition; (2) All sites record a disappearance of sinistral *G. truncatulinoides* over the interval MIS 21-15 (~850-600 kya); and (3) Variations in the coiling ratio of *G. truncatulinoides* over the course of this study interval are more frequent than the glacial-interglacial background at the southern sites closer to the gyre.
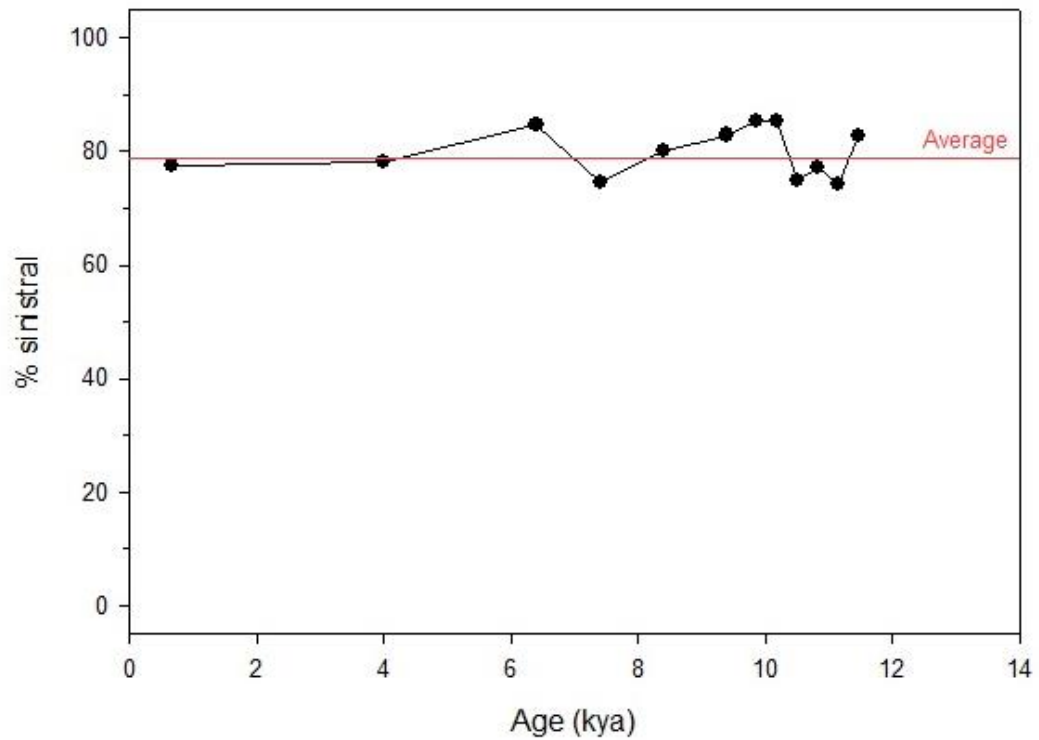
Figure 7.   Core-top sediment results from Site 1058 representing the most recent
interglacial period MIS 1 (the Holocene). The range of sinistral *G.
truncatulinoides* is between 74-86%, with an average of 79%. These
results are consistent with the distribution pattern observed by Ericson et
al. (1954) and Ujjié et al. (2010).
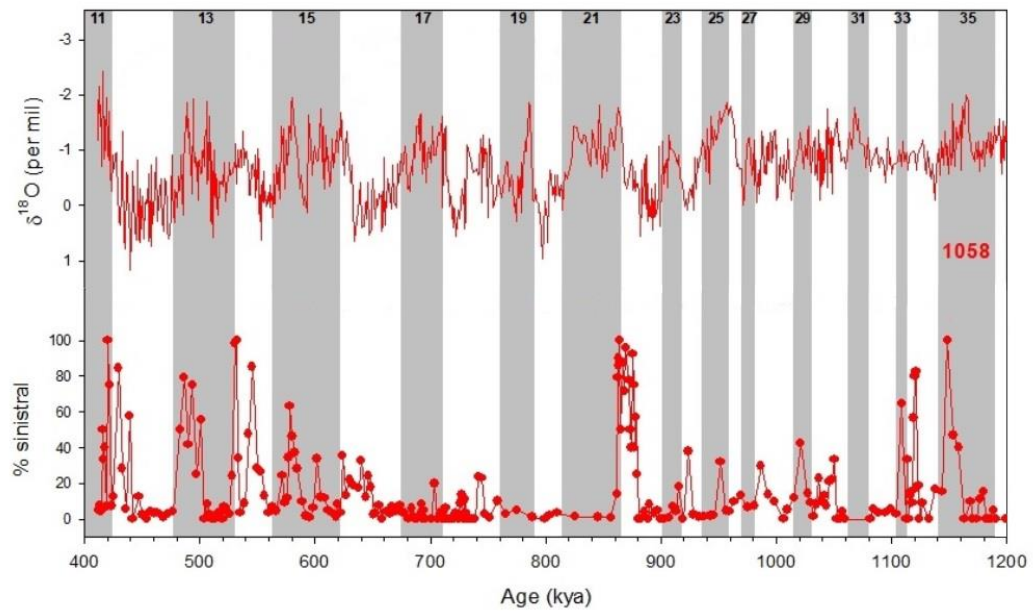
Figure 8.   Bottom panel shows the percent *Globorotalia truncatulinoides* (sinistral) from 400 ka to 1200 ka at Site 1058. Top panel shows the $\delta^{18}O$ record at Site 1058, representing the background climate. Vertical grey boxes represent interglacial Marine Isotope Stages and are labeled across the top.
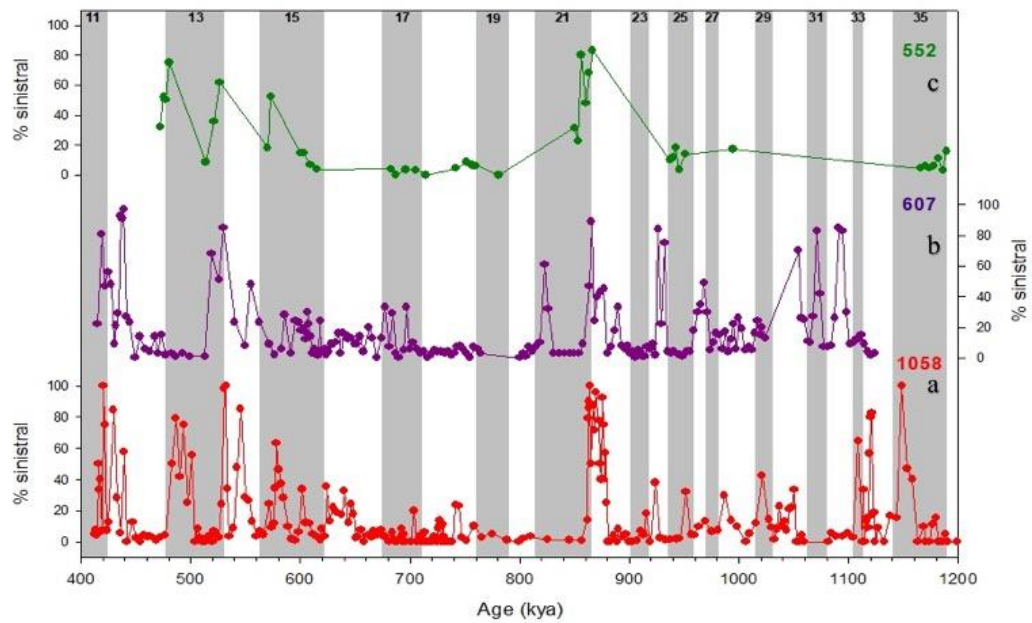
Figure 9.   Percent sinistral *G. truncatulinoides* from 400 ka to 1200 ka at (a) Site 1058 (red), (b) Site 607 (purple), and (c) Site 552 (green). Vertical grey boxes represent interglacial Marine Isotope Stages and are labeled across the top.

Chapter 6

DISCUSSION

6.1   Mid-Pleistocene Transition: MIS 23-21

A particular interval of interest during the MPT is its mid-point, MIS 23-21 (917-814 kya). Across this interval, all three sites in this study record a similar pattern of dextral *G. truncatulinoides* dominance, then a prominent, but short-lived peak in sinistral *G. truncatulinoides* dominance, followed by an extended disappearance of sinistral *G. truncatulinoides*. During the relatively cool interglacial MIS 23 (900 kya-917 kya), all three sites record minima in sinistral *G. truncatulinoides* (Figure 9). The dextral variety prefers the cooler, relatively nutrient-rich waters characteristic of gyre margins, which commonly, but not always, results in the dominance of the dextral variety in sediments during a glacial period (Renaud and Schmidt, 2003; Billups et al., 2016). Despite the fact that MIS 23 was an interglacial period, the $\delta^{18}O$ record shows that it was not as strong compared to MIS 25 and 21 (Figure 6). This is supported by the observation that thermohaline circulation was considerably weaker during this time (Raymo et al., 1997; Pena and Goldstein, 2014; Poirier and Billups, 2014). These observations, as well as the coiling ratio data, show that during the cooler, glacial-like conditions of MIS 23, dextral *G. truncatulinoides* dominate at the three sites in this study.

As interglacial MIS 23 ends and glacial MIS 22 begins (~900-880 kya), Sites 1058 and 607 continue to be dominated by minimal counts of sinistral *G. truncatulinoides* (Figure 9). The sample from Site 552 was not considered for this time

interval because there was only one single test found. This lack of sinistral *G. truncatulinoides* is generally observed during a glacial interval, as shown by Feldmeijer et al. (2014) and Billups et al. (2016). During MIS 22, thermohaline circulation was weak, which is a characteristic of glacial periods (Raymo et al., 1997; Pena and Goldstein, 2014; Poirier and Billups, 2014). This would be consistent with a weaker Gulf Stream and much less of a contribution of the North Atlantic Current to the formation of North Atlantic Deep Water, which would be further enforced by a southward movement of the Arctic Front (Naafs et al., 2010; Alonso-Garcia et al, 2011; Poirier and Billups, 2014). These oceanic conditions characteristic of the gyre margins favor dextral *G. truncatulinoides* and explain why very few sinistral *G. truncatulinoides* are present at the study sites (Figure 10).

During the transition from glacial MIS 22 to interglacial MIS 21 (~870 kya), all three sites had a maxima in sinistral *G. truncatulinoides* (Figure 9). The sinistral variety prefer the warmer, relatively nutrient-depleted waters characteristic of the center of the subtropical ocean gyre, which commonly results in the dominance of the sinistral variety in sediments during interglacial periods (Renaud and Schmidt, 2003; Feldmeijer et al., 2014; Billups et al., 2016). During this particular time, the central waters of the subtropical ocean gyre would have had much more of an influence in this area of the North Atlantic, which resulted in conditions favoring sinistral *G. truncatulinoides* (Figure 11). Assuming that a strengthening of the thermohaline circulation system caused the transition into this interglacial, strengthening of the Gulf Stream and the North Atlantic Current would also be expected (Pena and Goldstein, 2014; Poirier and Billups, 2014). In order for these currents to transport more warm water to the polar sites, the Arctic Front would have needed to move northward (Naafs

et al., 2010; Alonso-Garcia et al, 2011). These conditions are supported by the observations of maxima in sinistral *G. truncatulinoides* at all three sites, potentially recording the strengthening of the thermohaline circulation system (Figure 11).

As MIS 21 ends, the $\delta^{18}O$ record shows a return to glacial conditions (Figure 6). This would be consistent with a weakening of the Gulf Stream and North Atlantic Current, which would be coincident with a southward shift in the Arctic Front, limiting the ability of the warm salty waters of the subtropical North Atlantic to travel north (Naafs et al., 2010; Alonso-Garcia et al, 2011; Poirier and Billups). The sites would be more influenced from polar waters and waters from the gyre margins, which again favors dextral *G. truncatulinoides* (Figure 12). This is observed in the coiling ratio data, as Sites 1058 and 552 resume the disappearance of sinistral *G. truncatulinoides*. Site 607 also records a minimum in sinistral *G. truncatulinoides*, although there is a sudden but brief event where sinistral *G. truncatulinoides* are dominant (Figure 9b).

These observations match well with other studies tracking North Atlantic Deep Water export across the mid-Pleistocene transition. Prior to MIS 25, variability in NADW export was small between glacials and interglacials, and glaciations were paced at 41-kyr cycles (Raymo et al., 1997; Pena and Goldstein, 2014; Poirier and Billups, 2014). This appears to not have had much of an influence on the coiling direction of *G. truncatulinoides* during this interval as our results show that the coiling ratios were extremely variable between the three sites (Figure 9). After MIS 21, thermohaline circulation during glacial periods became much weaker, and we subsequently observed the development of 100-kyr glacial cycles (Raymo et al., 1997; Pena and Goldstein, 2014; Poirier and Billups, 2014). In the absence of any change in

orbital forcing, this change in glacial periodicity is attributed to changes in the climate system and its subsequent feedback loops, involving ice sheets, sea ice, and atmospheric CO_2 (Imbire et al., 1993; Raymo et al., 1997; Clark et al., 2006; Pena and Goldstein, 2014; Poirier and Billups, 2014).

Our results are consistent with findings of Naafs et al. (2010) and Alonso-Garcia et al. (2011), who emphasized the relationship between the North Atlantic Current (NAC) and the Arctic Front, and the impact this has on the hydrography of the polar North Atlantic across the mid-Pleistocene transition. Put simply, the position of the NAC is determined by the Arctic Front. The orientation (West-East or North-South) of the NAC ultimately influences which water mass is dominant in this area, which determines other conditions, including sea surface temperatures and nutrient concentrations. These changes through time should be recorded in the coiling ratio of *G. truncatulinoides*. For example, a strong NAC (North-South orientation) implies strong global thermohaline circulation, which means more warm, nutrient-depleted water from the subtropical gyre is being transported to the poles - these conditions favor the dominance of sinistral *G. truncatulinoides*. These conditions are characteristic of an interglacial. Conversely, a weak NAC (West-East orientation) implies weak global thermohaline circulation, which means that less heat is being transported to the poles and cooler, nutrient-rich polar waters are dominant. These conditions are characteristic of a glacial period and favor dextral *G. truncatulinoides*. With this in mind, it becomes possible to infer the upper ocean hydrography of the study site based on the coiling ratio data collected from the sites in this study.

As mentioned above, during MIS 23, global thermohaline circulation was considerably weak compared to a "normal" interglacial (Raymo et al., 1997; Pena and

Goldstein, 2014; Poirier and Billups, 2014). This is a particularly important interval because most interglacials tend to record a strengthening of this circulation, suggesting that whatever caused this structural shift in hydrography contributed to the stabilization and persistence of the more intense glaciations characteristic of the current "100-kyr year world" (Boyle and Keigwin, 1982; Clark et al., 2006; Alonso-Garcia et al., 2011; Pena and Goldstein, 2014; Poirier and Billups, 2014). This observation also provides an explanation as to why MIS 23 was much colder than most other interglacials. After this unique period, MIS 21 shows a return to "normal" interglacial conditions (Figure 6), implying an increase in the global ocean circulation system. By MIS 17, export of North Atlantic Deep Water strengthens, resulting in a circulation pattern similar to the modern, which is observed in many deep-ocean circulation reconstructions and faunal assemblages (Alonso-Garcia et al., 2011; Pena and Goldstein, 2014; Poirier and Billups, 2014). Our results support these observations because the peak in left coiling tests at the northernmost site during MIS 22/21 suggests enhanced warm water advection to this polar region of the North Atlantic. But, if this maxima in sinistral G. *truncatulinoides* actually does represent changes in hydrography resulting from this thermohaline circulation event, it is interesting as to why the next few hundred-thousand years are dominated by dextral G. *truncatulinoides*.

6.2   Disappearance of sinistral *G. truncatulinoides*

All three sites in this study record an ~300 kyr disappearance of sinistral *G. truncatulinoides* after the mid-Pleistocene transition (Figure 6). At Site 552, this pattern is fairly predictable, as core-top sediments from this high latitude site tend to be dominated by dextral *G. truncatulinoides* (Ericson et al., 1955; Ujiié et al., 2010).

39

But at the more subtropical Sites 607 and 1058, this pattern is somewhat unusual, considering that many other studies have observed some sort of climatic (glacial-interglacial) or astronomical (precession and obliquity) cyclicity in the coiling ratio of *G. truncatulinoides* during much of the post-MPT, "100 kyr world" (Ufkes and Kroon, 2012; Feldmeijer et al., 2014; Billups et al., 2016). The sudden reappearance and periodic dominance of sinistral *G. truncatulinoides* at these sites beginning ~600 kya and occurring into the modern is also an interesting feature observed in other studies (Ufkes and Kroon, 2012). It is around this time that the current 100-kyr glacial cycle is thought to have been well established (Mudelsee and Schulz, 1997; Clark et al., 2006), leading to the question: Why are these patterns observed, and how are they related to climate development across the mid-Pleistocene transition?

This disappearance of sinistral *G. truncatulinoides* is not unique to the subtropical North Atlantic and has in fact been observed at several locations in the South Atlantic (Cullen and Curry, 1997; Ufkes and Kroon, 2012). Cullen and Curry (1997) observe a disappearance of sinistral *G. truncatulinoides* between MIS 24-16 (930-670 kya), but do not propose a reason for the absence (Cullen and Curry, 1997). Ufkes and Kroon (2012) observed the disappearance of this morphotype to be coincident with the cooling of surface and deeper waters during MIS 26 (970-959 kya) (Ufkes and Kroon, 2012). This cooling was suggested to have occurred due to changes in ocean mixing in this region during the beginning of the mid-Pleistocene transition.

The disappearance of sinistral *G. truncatulinoides* in the North Atlantic did not occur until MIS 21 (~870 kya; Figure 9). Similar to Ufkes and Kroon (2012), the reappearance of sinistral *G. truncatulinoides* in the North Atlantic occurred during MIS 15 (~600 kya; Figure 9). The inconsistency between the timing of the

disappearance and reappearance of sinistral *G. truncatulinoides* in the North and South Atlantic suggest that there were differences in oceanic conditions in the South Atlantic compared to the North Atlantic that had an influence on the coiling direction of *G. truncatulinoides*.

Individual water masses have specific hydrographic parameters (temperature, salinity, density, and nutrient concentration) that differentiate them from other water masses (Ottens, 1991). Based on the current knowledge of the life cycle of *G. truncatulinoides* (Bé, 1977; Lohmann and Schweitzer, 1990), it is reasonable to assume that changes in hydrographic parameters of certain water masses influence the organisms living in that environment, whether that be through morphology, genetics, or faunal assemblages. There is clearly some sort of extra-regional pattern occurring that challenges our interpretation of how changes in the coiling direction of *G. truncatulinoides* can be linked to certain oceanographic factors such as water masses or circulation.

6.3   Frequency in variation of sinistral *G. truncatulinoides*

Previous studies exploring the use of *G. truncatulinoides* as a paleoceanographic indicator have shown trends in the dominance of sinistral *G. truncatulinoides* on glacial-interglacial timescales. In the South Atlantic, Ufkes and Kroon (2012) observed dominance of dextral *G. truncatulinoides* during interglacials and dominance of sinistral G. truncatulinoides during glacials over the past 600 kyr. Billups et al. (2016) found a relationship between the dominance of sinistral *G. truncatulinoides* and both Northern and Southern hemisphere precession maxima (half precession cycles) in the subtropical North Atlantic over the last 280 kyr. Although that study generally observed more sinistral *G. truncatulinoides* during interglacials,

the relationship did not necessarily translate to a constant glacial-interglacial trend, as observed by Ufkes and Kroon (2012). MIS 8 (300-243 kya), 7 (243-191 kya), 6 (191-130 kya), and 2 (29-14 kya) were all instances where the variation in coiling direction of *G. truncatulinoides* was more frequent than the glacial-interglacial climate background (Billups et al., 2016). This frequency in variation of sinistral *G. truncatulinoides* is consistent with the present study. Because of the lack of pronounced variations in sinistral *G. truncatulinoides* between MIS 21-15 (870-600 kya), the time intervals that do show pronounced variation before (MIS 35-22 (1200-870 kya) and after (MIS 15-11, 600-400 kya) are not long enough to be certain whether the variations are link to any particular orbital cycle.

The lack of long-term patterns of dominance of sinistral *G. truncatulinoides* as well as the frequency of variation of the coiling ratio compared to the glacial-interglacial background climate lead to the idea that millennial-scale variations cannot be clearly distinguished by the time steps used in this study. The length of the marine isotope stages in this study interval range from 10-58 kyr. The samples counted in this study were picked at 20-40 cm intervals, which resulted in time steps of 2000-4000 years. It is possible that the resolution of some intervals may have been higher than others, which could hide some of the variations throughout the study interval. For example, if some of the shorter marine isotope stages were sampled at the same intervals as the longer stages, then those shorter stages would be greatly undersampled in comparison. This would hide some of the true variability throughout the study interval and could only be resolved through more frequent selection of sampling intervals.
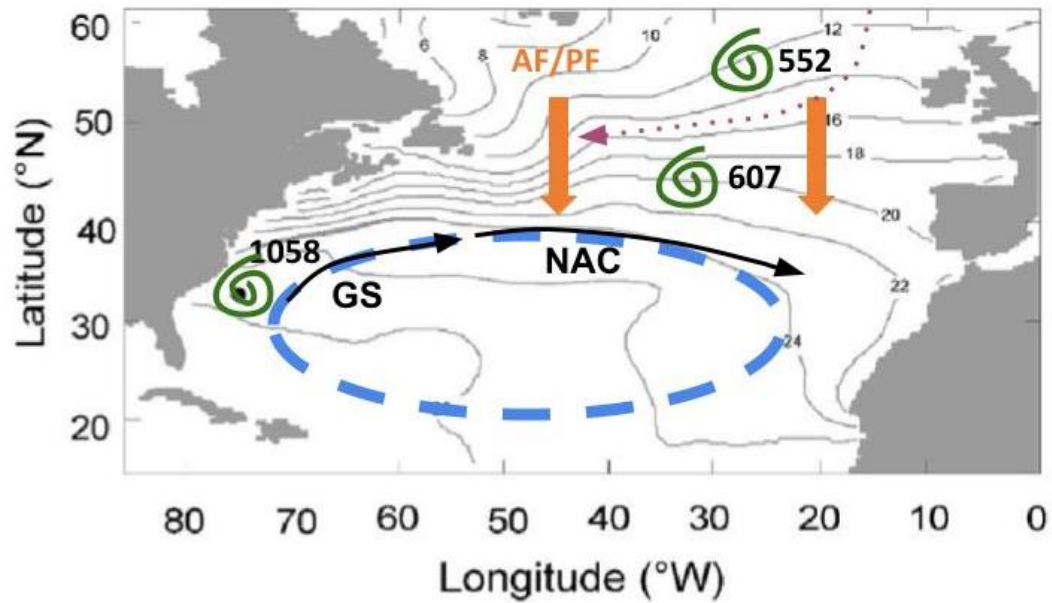
Figure 10.   Schematic of current flow in the North Atlantic during glacial MIS 22
              and the dominant variety of *G. truncatulinoides* observed at each site
              based on the hydrographic conditions. Green spirals represent dominance
              of dextral *G. truncatulinoides*. Blue dashed circle represents the North
              Atlantic gyre. Black dashed arrows represent currents (GS = Gulf
              Stream; NAC = North Atlantic Current). Purple dotted line represents
              North Atlantic Deep Water. Orange arrows represent the relative
              movement of the Arctic Front (AF). Study sites are labelled and are
              represented by the spirals.
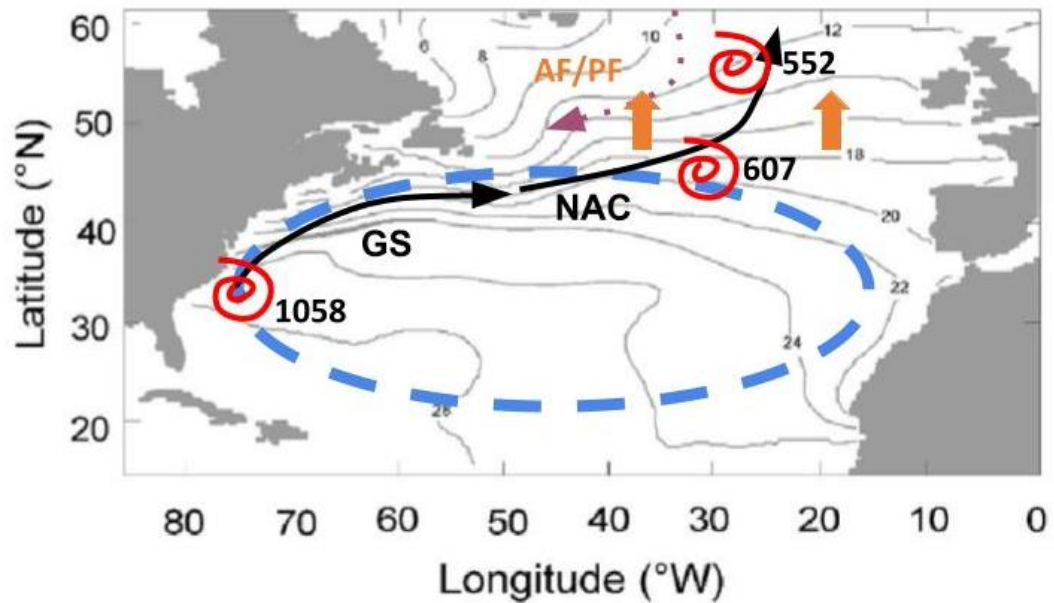
Figure 11.   Schematic of current flow in the North Atlantic during the transition from glacial MIS 22 to interglacial MIS 21 and the dominant variety of *G. truncatulinoides* observed at each site based on the hydrographic conditions. Red spirals represent dominance of sinistral *G. truncatulinoides*. Blue dashed circle represents the North Atlantic gyre. Black dashed arrows represent currents (GS = Gulf Stream; NAC = North Atlantic Current). Purple dotted line represents North Atlantic Deep Water. Orange arrows represent the relative movement of the Arctic Front (AF). Study sites are labelled and are represented by the spirals.
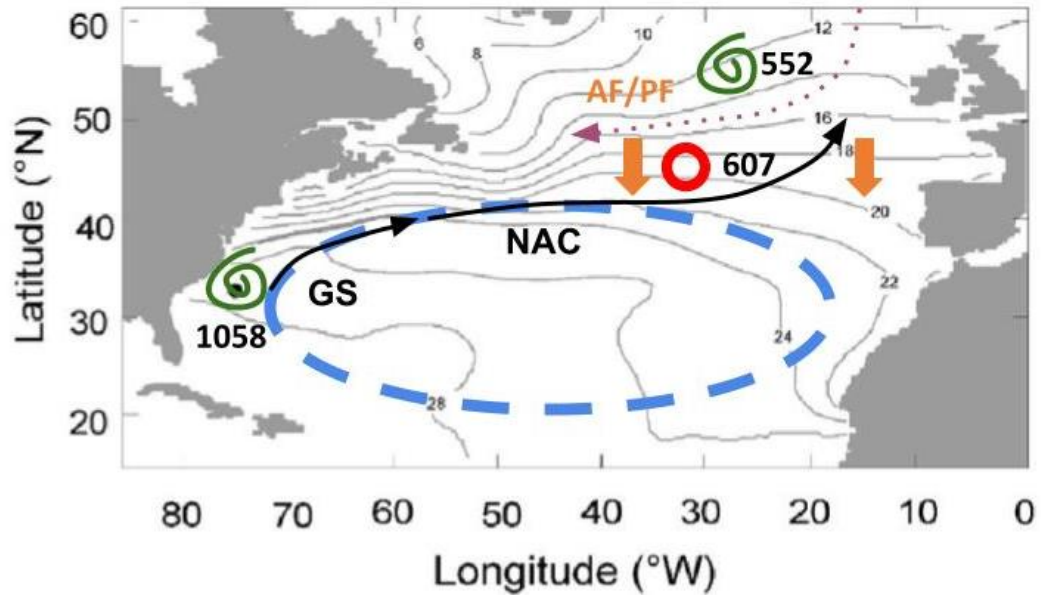
Figure 12.   Schematic of current flow in the North Atlantic during the end of
interglacial MIS 21 and the dominant variety of *G. truncatulinoides*
observed at each site based on the hydrographic conditions. Green spirals
represent dominance of dextral *G. truncatulinoides*. Thick red circles
represent dominance of neither variety. Blue dashed circle represents the
North Atlantic gyre. Black dashed arrows represent currents (GS = Gulf
Stream; NAC = North Atlantic Current). Purple dotted line represents
North Atlantic Deep Water. Orange arrows represent the relative
movement of the Arctic Front (AF). Study sites are labelled and are
represented by the spirals.

Chapter 7

CONCLUSION

The aim of this study was to construct a record of the coiling ratio of *G. truncatulinoides* at Site 1058 and compare it to coiling ratios at other sites in the North Atlantic to test whether changes in the relative position of the Gulf Stream and subtropical gyre and associated northward heat transport had an influence in the onset and establishment of the post-MPT, 100-kyr glacial cycles characteristic of the past 600 kyr. There are a few key findings most pertinent to this goal: (1) Around ~865 kya (MIS 21), all three sites in this study recorded a major peak (at least 80%) in the dominance of sinistral *G. truncatulinoides*; (2) All sites recorded a prolonged disappearance of sinistral *G. truncatulinoides* over the interval MIS 21-15 (~850-600 kya); and (3) Variations in the coiling direction of *G. truncatulinoides* at these three sites over the course of this study interval were more frequent than the glacial-interglacial background.

The dominance of sinistral *G. truncatulinoides* during MIS 21 supports previous studies that have reconstructed surface ocean circulation patterns across the mid-Pleistocene transition. Pena and Goldstein (2014) and Poirier and Billups (2014) both recorded a strengthening of the global thermohaline circulation system, which was further supported by reconstructions of the movement of the Arctic Front by Naafs et al. (2010) and Alonso-Garcia et al. (2011) across the same time interval. These findings suggest that the hydrographic conditions in this region during this time

were favorable for the presence and dominance of sinistral *G. truncatulinoides*, which is proven by the coiling ratio data (Figure 9).

The ubiquity of this particular instance of sinistral *G. truncatulinoides* dominance as well as the disappearance of sinistral *G. truncatulinoides* at all three sites in this study suggests that all three sites are influenced by changes in the upper ocean hydrography of this region. A similar study by Ufkes and Kroon (2012) showed an even longer disappearance of sinistral *G. truncatulinoides* at several different sites in the South Atlantic. Therefore, it is clear that changes in the coiling direction of *G. truncatulinoides* are sensitive to hydrographic changes on extra-regional spatial scales.

The frequency in variation of the coiling direction of *G. truncatulinoides* in this study was much greater than the glacial-interglacial climate background, especially when compared to previous studies. Ufkes and Kroon (2012) report a consistent pattern of dextral *G. truncatulinoides* during interglacials and sinistral *G. truncatulinoides* during glacials. Billups et al. (2016) observed a less consistent but still noticeable glacial-interglacial pattern of sinistral *G. truncatulinoides* dominance and disappearance, although this study found sinistral *G. truncatulinoides* dominant during interglacials and dextral *G. truncatulinoides* dominant during glacials. Feldmeijer et al. (2014), over a much shorter study interval, did not observe any correlation between the coiling ratio *G. truncatulinoides* and the glacial-interglacial climate background. The overall variation in the coiling ratio of *G. truncatulinoides* was much more frequent than glacial-interglacial cycles, suggesting that this proxy is extremely sensitive on timescales smaller than glacial-interglacial cycles.

This study contributes to the larger body of research that uses the morphological variations of *G. truncatulinoides* through time to gain useful

paleoceanographic information. We find that on the smaller scale, singular events can provide additional evidence for paleoceanographic changes in hydrography. On the larger scale, this method of research can show relationships across the latitudinal gradient of an entire ocean basin. Using this species as a paleoceanographic indicator is a field of study that should continue to grow and refine itself the more it is used.

REFERENCES

Alonso-Garcia, M., Sierro, F. J., & Flores, J. A. (2011). Arctic front shifts in the subpolar North Atlantic during the Mid-Pleistocene (800–400ka) and their implications for ocean circulation. *Palaeogeography, Palaeoclimatology, Palaeoecology*, *311*(3), 268-280.

Balch, W. M., P. M. Holligan, and K. A. Kilpatrick (1991), Calcification, photosynthesis and growth of the bloom-forming coccolithophore, *Emiliania huxleyi, Cont. Shelf Res., 12 (12)*, 1353-1374.

Barker, S., and H. Elderfield (2002), Foraminiferal calcification response to glacial-interglacial changes in atmospheric CO_2, *Science, 297*, 883-836.

Bé, A. W. H. (1960), Ecology of recent planktonic foraminifera: Part 2—Bathymetric and seasonal distributions in the Sargasso Sea off Bermuda, *Micropaleontology*, 6 (4), 373–392.

Bé, A. W. H. (1977), An ecological, zoogeographic, and taxonomic review of recent planktonic foraminifera, in *Oceanic Micropalaeontology*, edited by A. T. S. Ramsay, pp. 1–100, Academic Press, London.

Berger, A., et al. (eds.), Milankovitch and Climate, Part 1, 269-305 (1984).

Berger, A., X. S. Li, and M. F. Loutre (1999), Modelling northern hemisphere ice volume over the last 3 Ma, *Quat. Sci. Rev., 18*, 1-11.

Billups, K., C. Hudson, H. Kunz, and I. Rew (2016), Exploring *Globorotalia truncatulinoides* coiling ratios as a proxy for subtropical gyre dynamics in the northern Atlantic Ocean during the late Pleistocene Ice Ages, *Paleoceanography, 31*, doi:10.1002/2016PA002927.

Boyle, E. A., & Keigwin, L. D. (1982). Deep circulation of the North Atlantic over the last 200,000 years: Geochemical evidence. *Science*, *218*(4574), 784-787.

Carlson, A. E., Oppo, D. W., Came, R. E., LeGrande, A. N., Keigwin, L. D., Curry, W. B. (2008), Subtropical Atlantic salinity variability and Atlantic meridional circulation during the last deglaciation, *Geology*, 36 (12), 991-994.

Clark, P. U., and D. Pollard (1998), Origin of the middle Pleistocene transition by ice sheet erosion of regolith, *Paleoceanography, 13* (1), 1-9.

Clark, P.U., D. Archer, D. Pollard, J. D. Blum, J. A. Rial, V. Brovkin, A. C. Mix, N. G. Pisias, and M. Roy (2006), The middle Pleistocene transition: characteristics, mechanisms, and implication for long-term changes in atmospheric pCO₂, *Quat. Sci. Rev., 25*, 3150-3184.

Cléroux, C., E. Cortijo, and J. Duplessy (2007), Deep-dwelling foraminifera as thermocline temperature recorders, *Geochem. Geophys. Geosyst., 8*, Q04N11, doi:10.1029/2006GC001474.

Cléroux, C., J. Lynch-Stieglitz, M. W. Schmidt, E. Cortijo, and J. Duplessy (2009), Evidence for calcification depth changes of *Globorotalia truncatulinoides* between deglaciation and Holocene in the Western Atlantic Ocean, *Mar. Micropaleontol., 73*, 57-61.

Cullen, J. L., & Curry, W. B. (1997). Variations in planktonic foraminifer faunas and carbonate preservation at site 927: evidence for changing surface water conditions in the Western Tropical Atlantic Ocean during the middle Pleistocene. In *Proceedings of the Ocean Drilling Program. Scientific Results*(Vol. 154, pp. 207-228). Ocean Drilling Program.

De Vargas, C., S. Renaud, H. Hilbrecht, and J. Pawlowski (2001), Pleistocene adaptive radiation in *Globorotalia truncatulinoides*: Genetic, morphologic, and environmental evidence, *Paleobiology, 27*, 104-125.

Duplessy, J. C., Shackleton, N. J., Fairbanks, R. G., Labeyrie, L., Oppo, D., & Kallel, N. (1988). Deepwater source variations during the last climatic cycle and their impact on the global deepwater circulation. *Paleoceanography*, *3*(3), 343-360.

Ericson, D., G. Wollin, and J. Wollin (1954), Coiling direction of *Globorotalia truncatulinoides* in deep-sea cores, *Deep Sea Res., 2*, 152-158.

Emiliani, C. (1955). Pleistocene temperatures. *The Journal of Geology*, *63*(6), 538-578.

Feldmeijer, W., B. Metcalfe, G. Brummer, and G. Ganssen (2014), Reconstructing the depth of the permanent thermocline through the morphology and geochemistry of the deep dwelling planktonic foraminifer *Globorotalia truncatulinoides, Paleoceanography, 30*, 1-22, doi:10.1002/2014PA002687.

Gersonde, R., D. A. Hodell, and P. Blum (1999), Proceedings of the Ocean Drilling Program, Initial Reports, vol. *177*, pp. 1-101.

Hays, J.D., J. Imbrie, N. J. Shackleton (1976), Variations in the Earth's orbit: pacemaker of the ice ages, *Science,* 194, 1121–1132.

Healy-Williams, N. (1983), Fourier shape analysis of *Globorotalia truncatulinoides* from late Quaternary sediments in the southern Indian Ocean, *Mar. Micropaleontol., 8* (1), 1-15.

Healy-Williams, N., Ehrlich, R., & Williams, D. F. (1985). Morphometric and stable isotopic evidence for subpopulations of Globorotalia truncatulinoides. *The Journal of Foraminiferal Research*, *15*(4), 242-253.

Hemleben, C., M. Spindler, and O. R. Anderson (1989), *Modern Planktonic Foraminifera*, 363 pp., Springer, New York.

Hodell, D. A., K. A. Venz, C. D. Charles, and U. S. Ninnemann (2003), Pleistocene vertical carbon isotope and carbonate gradients in the South Atlantic sector of the Southern Ocean, *Geochem. Geophys. Geosyst., 4* (1), 1004, doi:10.1029/2002GC000367.

Imbrie, J., A. Berger, E. A. Boyle, S. C. Clemens, A. Duffy, W. R. Howard, G. Kukla, J. Kutzbach, D. G. Martinson, A. McIntyre, A. C. Mix, B. Molfino, J. J. Morley, L. C. Peterson, N. G. Pisias, W. L. Prell, M. E. Raymo, N. J. Shackleton, J. R. Toggweiler (1993), On the structure and origin of major glaciation cycles 2. The 100,000-year cycle, *Paleoceanography*, 8 (6), 699-735.

Jansen, E. (1989). The use of stable oxygen and carbon isotope stratigraphy as a dating tool. *Quaternary International*, *1*, 151-166.

Kaiser, E., Caldwell, A., and K. Billups (2018), Using coiling ratios of planktonic foraminifera to trace past North Atlantic surface currents during the Mid Pleistocene Transition.

Keigwin, L. D., D. Rio, and G. D. Acton (1998), Proceedings of the Ocean Drilling Program, Initial Reports, vol. *172*, pp. 77-156.

Kroopnick, P. M. (1985). The distribution of 13C of ΣCO2 in the world oceans. *Deep Sea Research Part A. Oceanographic Research Papers*, *32*(1), 57-84.

Lear, C.H., K. Billups, R. E. M. Rickaby, L. Diester-Haass, E. M. Mawbey, and S. Sosdian (2016), Breathing more deeply: Deep ocean carbon storage during the mid-Pleistocene climate transition, *Geology,* 1-4.

Lisiecki, L. E., and M. E. Raymo (2005), A Pliocene-Pleistocene stack of 57 globally distributed benthic δ^{18}O records, *Paleoceanography*, 20, PA1003, doi:10.1029/2004PA001071.

Lohmann, G., and P. Schweitzer (1990), *Globorotalia truncatulinoides'* growth and chemistry as probes of the past thermocline: 1. Shell size, *Paleoceanography, 5*, 55-75, doi:10.1029/PA005i001p00055.

Lohmann, G.P. (1992), Increasing seasonal upwelling in the subtropical South Atlantic over the past 700,000 yrs: Evidence from deep-living planktonic foraminifera. In: G.J. van der Zwaan, F.J. Jorissen and W.J. Zachariasse (Editors), Approaches to Paleoproductivity Reconstructions. *Mar. Micropaleontol.,* 19:1-12.

Lund, D. C., J. Lynch-Stieglitz, and W. B. Curry (2006), Gulf Stream density structure and transport during the past millennium, *Nature, 444*, 601-604.

Matsumoto, K., and J. Lynch-Stieglitz (2003), Persistence of Gulf Stream separation during the Last Glacial Period: Implications for current separation theories, *J. Geophys. Res., 108*(C6), 3174, doi:10.1029/2001JC000861, 2003.

Milankovitch, M. M., Théorie Mathématique des Phénomènes Thermiques Produits par la Radiation Solaire, Academie Yougoslave des Sciences et des Arts de Zagreb, Gauthier-Villars, Paris, 1920.

Mudelsee, M., and M. Schulz (1997), The Mid-Pleistocene climate transition: onset of 100 ka cycle lags ice volume build-up by 280 ka, *EPSL, 151*, 117-123.

Naafs, B. D. A., Stein, R., Hefter, J., Khélifi, N., De Schepper, S., & Haug, G. H. (2010). Late Pliocene changes in the North Atlantic current. *Earth and Planetary Science Letters*, *298*(3), 434-442.

Oerlemans, J. (1991), The role of ice sheets in the Pleistocene climate, *Norsk Geologist Tidsskrift, 71*, 155-161.

Oppo, D. W., and R. G. Fairbanks (1987), Variability in the deep and intermediate water circulation of the Atlantic Ocean during the past 25,000 years: Northern Hemisphere modulation of the Southern Ocean, *EPSL, 86*, 1-15.

Ottens, J. J. (1991). Planktic foraminifera as North-Atlantic water mass indicators. *Oceanologica Acta*, *14*(2), 123-140.

Pälike, H., 2003. Practical: Milankovitch theory and its applications.

Pena, L. D., and S. L. Goldstein (2014), Thermohaline circulation crisis and impacts during the mid-Pleistocene transition, *Science, 345*, 318-322.

Petit, J. R., J. Jouzel, D. Raynaud, N. I. Barkov, J. -M. Barnola, I. Basile, M. Bender, J. Chappellaz, M. Davis, G. Delaygue, M. Delmotte, V. M. Kotlyakov, M. Legrand, V. Y. Lipenkov, C. Lofius, L. Pépin, C. Ritz, E. Saltzman, and M. Stievenard (1999), Climate and atmospheric history of the past 420,000 years from the Vostok ice core, Antarctica, *Nature, 399*, 429-436.

Pisias, N. G., and T. C. Moore, Jr. (1981), The evolution of Pleistocene climate: a time series approach, *EPSL, 52*, 450-458.

Poirier, R. K., and K. Billups (2014), The intensification of northern component deepwater formation during the mid-Pleistocene climate transition, *Paleoceanography, 29*, doi:10.1002/ 2014PA002661.

Raymo, M. E., W. F. Ruddiman, J. Backman, B. M. Clement, and D. G. Martinson (1989), Late Pliocene variations in Northern Hemisphere ice sheets and North Atlantic deep water circulation, *Paleoceanography, 4* (4), 413-446.

Raymo, M. E., W. F. Ruddiman, N. J. Shakleton, and D. W. Oppo (1990), Evolution of Atlantic-Pacific δ^{13}C gradients over the last 2.5 m.y., *EPSL, 97*, 353-368.

Raymo, M. E., D. W. Oppo, and W. Curry (1997), The mid-Pleistocene climate transition: a deep sea carbon isotope perspective, *Paleoceanography, 12* (4), 546-559.

Raymo, M. E., and K. Nisancioglu (2003), The 41 kyr world: Milankovitch's other unsolved mystery, *Paleoceanography, 18* (1), 1011, doi:10.1029/2002PA000791

Renaud, S., & Schmidt, D. N. (2003). Habitat tracking as a response of the planktic foraminifer Globorotalia truncatulinoides to environmental fluctuations during the last 140 kyr. *Marine Micropaleontology*, *49*(1-2), 97-122.

Roberts, D. G., Schnitker, D., et al., 1984. *Init. Repts. DSDP,* 81: Washington (U.S. Govt. Printing Office).

Ruddiman, W. F., Sarnthein, M., et al., 1988. *Init. Repts. ODP,* 108: Washington (U.S. Govt. Printing Office).

Ruddiman, W. F., M. E. Raymo, D. G. Martinson, B. M. Clement, and J. Backman (1989), Pleistocene evolution: Northern Hemisphere ice sheets and North Atlantic Ocean, *Paleoceanography, 4* (4), 353-412.

Ruddiman, W. F. (2008), Earth's Climate: Past and Future, W. H. Freeman and Company, New York.

Seager, R., D. S. Battisti, J. Yin, N. Gordon, N. Naik, A. C. Clement, and M. A. Cane (2002), Is the Gulf Stream responsible for Europes mild winters?, *Q. J. R. Meteorol. Soc., 128*, 2563-2586.

Schmitz, W. J., and M. S. McCarthy (1993), On the North Atlantic circulation, *J. Geophys. Res., 31*, 29-49.

Theide, J. (1971), Variations in coiling ratio of Holocene planktonic foraminifera, *Deep sea Res., 18*, 823-831.

Tolderlund, D. S., & Bé, A. W. (1971). Seasonal distribution of planktonic foraminifera in the western North Atlantic. *Micropaleontology*, 297-329.

Tziperman, E., and H. Gildor (2003), On the mid-Pleistocene transition to 100-kyr glacial cycles and the asymmetry between glaciation and deglaciation times, *Paleoceanography, 18 (1)*, 1-8.

Ufkes, E. L. S., & Kroon, D. (2012). Sensitivity of south-east Atlantic planktonic foraminifera to mid-Pleistocene climate change. *Palaeontology*, *55*(1), 183-204.

Ujjié, Y., T. de Gardiel-Thoron, S. Watanabe, P. Wiebe, and C. de Vargas (2010), Coiling dimorphism within a genetic type of the planktonic foraminifer *Globorotalia truncatulinoides*, *Mar. Micropaleontol., 77*, 145-153.

Venz, K. A., Hodell, D. A., Stanton, C., & Warnke, D. A. (1999). A 1.0 Myr record of Glacial North Atlantic Intermediate Water variability from ODP site 982 in the northeast Atlantic. *Paleoceanography*, *14*(1), 42-52.

Venz, K. A., and D. A. Hodell (2002), New evidence for changes in Plio-Pleistocene deep water circulation from Southern Ocean ODP Leg 177 Site 1090, *Palaeogeogr. Palaeoclimatol. Palaeoecol., 20* (4), 263-276.

Weertman, J. (1964), Rate of growth and shrinkage of non-equilibrium ice sheets, *Journal of Glaciology, 5*, 145-158.

Weirauch, D., K. Billups, and P. Martin (2008), Evolution of millennial-scale climate variability during the mid-Pleistocene, *Paleoceanography, 23*, 1-16.